

## Raman scattering of InAs/AlAs strained-layer superlattices

G. Armelles, M. Recio, J. M. Rodríguez, and F. Briones

Centro Nacional de Microelectronica, del Consejo Superior de Investigaciones Cientificas,  
Serrano 144, E-28006 Madrid, Spain

(Received 11 July 1989)

We report on the resonance behavior around the  $E_1$  optical gap of the confined phonons of InAs/AlAs strained-layer superlattices. Near such a gap both types of phonons ( $A_1, B_2$ ) resonate. We discuss their resonance and compare it with the behavior when exciting near the fundamental band-gap transition.

Strained-layer superlattices were the subject of much research work during recent years. In these artificial materials, together with the confinement effect already present in lattice-matched systems, there is another factor, strain, which determines the electronic and phonon properties. As far as the phonon properties are concerned, the main effect of strain is an energy shift with respect to the phonon energy of the constituent materials. This shift can be easily measured using a conventional Raman spectrometer. From the obtained values the internal strain in the layers can be derived.<sup>1-3</sup> In Raman experiments, the intensity of the scattered light is a function of the energy of the exciting beam. Much of the published work refers to the study of the resonant behavior around energy levels near the fundamental band gap.<sup>4,5</sup> There are few works published concerning the resonant excitation of the phonons around energy levels far from this fundamental band gap.<sup>6-8</sup> In this paper, we present resonant Raman experiments around the  $E_1$  transition of InAs/AlAs strained-layer superlattices. Optical transitions were determined by spectroscopic ellipsometry. Two transitions near the  $E_1$  and  $E_1 + \Delta_1$  transitions of InAs bulk material are observed in the InAs/AlAs superlattices studied. When scanning the energy of the exciting beam around these transitions, we observe a resonant behavior quite different from that reported for resonance near the fundamental band gap of superlattices. In this paper, we analyze in detail and discuss this behavior.

The samples studied were grown by atomic-layer molecular-beam epitaxy<sup>9</sup> on (001)-oriented GaAs substrates. In order to check the nominal superlattice growth parameters, the period was determined by x-ray diffraction and the mean composition by energy-dispersive analysis of the x-ray data. With this data we were able to determine the respective thicknesses of the constituent layers. These parameters are displayed in Table I. Raman spectra were obtained at room temperature and 77 K

with the back scattering geometry being the axes  $x = 100$ ,  $y = 010$ , and  $z = 001$ . The scattered light was analyzed by means of a double monochromator equipped with holographic gratings and detected with standard photon-counting techniques. The different lines of an Ar<sup>+</sup> laser were used as exciting beams.

In Fig. 1 we present Raman spectra for the two samples studied here. Because the optical-phonon branches of InAs and AlAs do not overlap, confined optical phonons are expected to be observed, similar to those present on GaAs/AlAs superlattices. As can be seen in Fig. 1, the energy position of the AlAs- and InAs-related optical phonons are shifted. The longest contribution to this shift is due to strain. The fact that both InAs and AlAs layers accommodate part of the total mismatch means that the critical thickness of the superlattice has been exceeded and it has its own lattice parameter, with a value between that of AlAs and InAs; so a network of misfit dislocations must have been generated in the region close to the

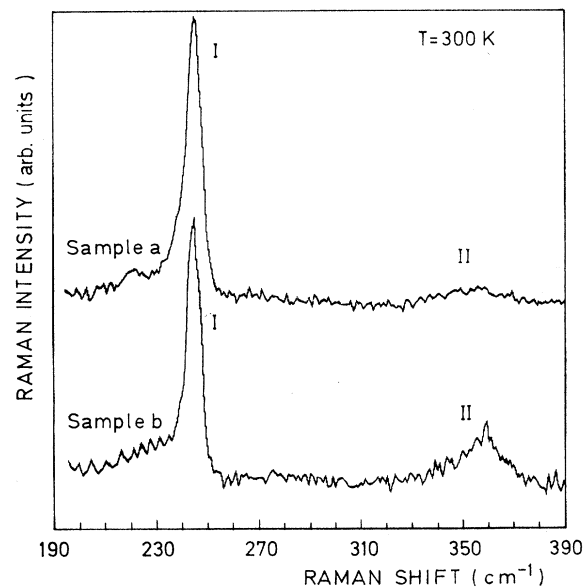


FIG. 1. Raman spectra of the two samples studied here. Peaks I and II refer to the InAs- and AlAs-related phonons, respectively. The strain-free energies of InAs and AlAs LO phonons are at 300 K  $238.6 \text{ cm}^{-1}$  and  $404.1 \text{ cm}^{-1}$ , respectively.

TABLE I. Sample parameters:  $d_1$  InAs layer thickness,  $d_2$  AlAs layer thickness. Energies of the  $E_1$  and  $E_1 + \Delta_1$  transitions.

	$d_1$ (Å)	$d_2$ (Å)	$E_1$ (eV)	$E_1 + \Delta_1$ (eV)
Sample a	42.7	5.0	2.55	2.845
Sample b	21.5	8.1	2.57	2.945

substrate-superlattice interface. We believe that the density of dislocations in the region near the surface sampled by Raman scattering is low because the full width at half maximum of the InAs-related phonon is equivalent to that of the InAs bulk material taken in the same experimental conditions ( $3 \text{ cm}^{-1}$ ) and also the intensity of the forbidden TO phonon is low (it should be pointed out that for the wavelength used here the penetration depth of the light is  $200 \text{ \AA}$  and the total thickness of the superlattices is  $4000 \text{ \AA}$ ).

Ellipsometry spectra for the samples under study are presented in Fig. 2. We observe two clear transitions. Their energy, as obtained by fitting from a second-derivative spectra, are presented in Table I (they are labeled  $E_1$  and  $E_1 + \Delta_1$  because they are near the same transitions for bulk InAs).

These transitions are located within a photon energy range where the exciting beam can be easily scanned by using the various discrete lines of an  $\text{Ar}^+$  laser. In doing so, we observe that, as we approach the energy of the transition, the scattered intensity of the InAs-related phonons increases, whereas the AlAs-related phonon intensity remains nearly constant. This means that the electrons involved in those transitions are confined in the InAs layers. Therefore, in the following we will deal only with the InAs-related phonons.

In Fig. 3 we present Raman spectra for the two samples at room temperature and near-resonance conditions. For the shortest period, sample *b*, we observe that the peaks detected on the  $Z(XY)\bar{Z}$  and  $Z(XX)\bar{Z}$  configurations, which correspond to the scattering by LO1 and LO2 phonons, respectively, do not overlap. On the other hand, for the other sample, *a*, the energy distance between both peaks decreases. The  $XX$  polarized spectrum in Fig. 3, corresponding to the longest period, sample *a*, shows a "shoulder" on the low-energy side of the LO2 phonon,

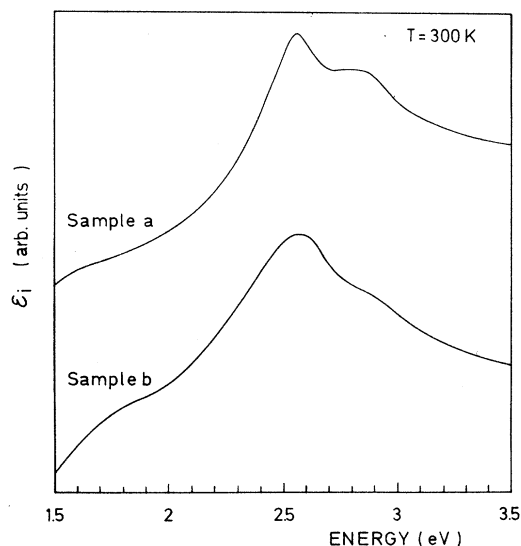


FIG. 2. Imaginary part of the pseudodielectric function ( $\epsilon_i$ ) of the samples studied here.

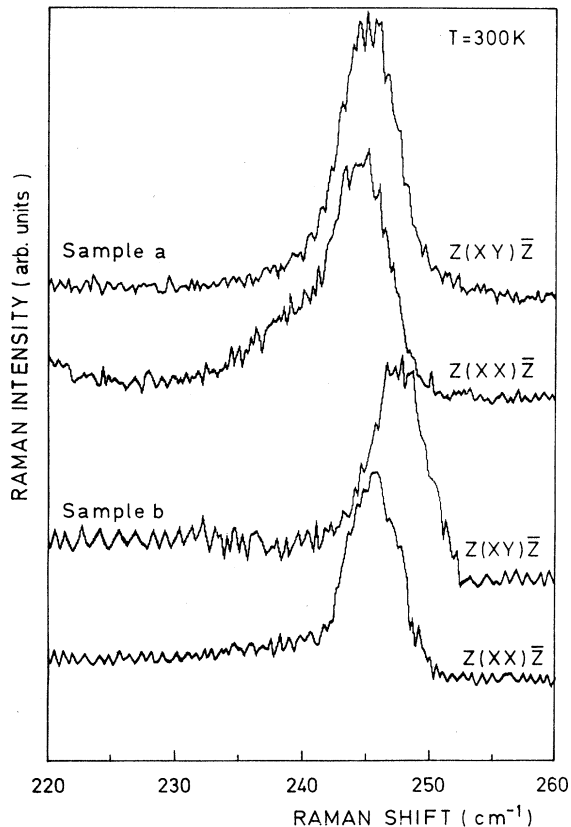


FIG. 3. Raman spectra of the samples *a* and *b* taken in the different back scattering configurations.

which we attribute to another confined phonon (LO4); this assignment is made on the basis of the following facts: At near-resonance conditions, the second-order spectrum of this sample (see Fig. 4) shows a sharp peak at an energy corresponding to the sum  $\omega_{\text{LO2}} + \omega_{\text{LO4}}$ . In the second-order spectrum, phonons with different momentum

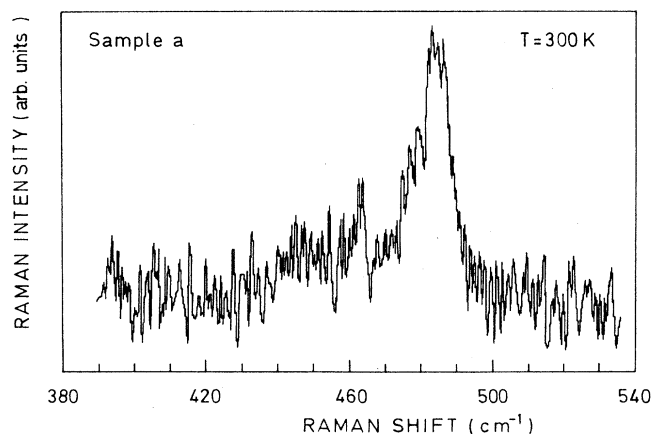


FIG. 4. Second-order Raman spectrum of sample *a* taken near resonance conditions.

can contribute to the scattering. If the mentioned "shoulder" in the first-order spectrum were originated by an interface phonon<sup>10</sup> (the other possible assignment) it should give a broader peak in the second-order spectrum, because the interface phonon shows a large dispersion in frequency with  $q$ . On the other hand,  $A_1$  symmetry phonons (like LO2 and LO4) are nearly dispersionless<sup>11,12</sup> and then will originate a sharper peak in the second-order spectrum.

In Fig. 5 we present the scattering intensity of the different confined phonons as a function of the energy of the incident radiation, normalized to that of the  $\text{CaF}_2$  phonon (the spectra were obtained at 77 K). These figures are not directly related to the Raman scattering efficiency because they are not corrected from the absorption coefficients. As expected from the ellipsometry measurements, we observe a displacement of the resonance towards higher energy as the period of the superlattices decreases. The resonance of the  $A_1$ -type phonons (LO2) are sharper than that of the  $B_2$  phonons (LO1) reflecting the different mechanisms of the electron-phonon interaction. This feature is observed in the two samples and from now on we will focus our discussion on the shortest-period sample, where the different phonons are well separated. Let us recall Fig. 3 where the resonance spectrum of sample  $b$  is presented. As can be seen, the  $B_2$ -type phonon (LO1) is only observed in the  $Z(XY)\bar{Z}$  configuration and the  $A_1$ -type phonon (LO2) is only observed in the  $Z(XX)\bar{Z}$  configuration, both phonons resonate. These facts are different from that observed near band gap, where  $B_2$ -type phonons hardly resonate and  $A_1$ -type phonons are seen in both configurations. This difference can be easily understood: The Raman efficiency is proportional to<sup>13</sup>

$$\left| \sum_{i,j} \frac{\langle 0 | \hat{\epsilon}_S \cdot \mathbf{p} | i \rangle \langle i | H_{e-p} | j \rangle \langle j | \hat{\epsilon}_L \cdot \mathbf{p} | 0 \rangle}{(\omega_L - \omega_j)(\omega_S - \omega_i)} \right|^2, \quad H_{e-p} = H_D + H_F, \quad (1)$$

where  $H_D$  represents the deformation potential interaction and  $H_F$  the Fröhlich interaction. In conditions of near resonance with the band gap ( $n=1$  heavy-hole-electron transition), the  $B_2$ -type phonons are hardly observed because the two factors in the denominator do not resonate at the same time [the deformation potential interaction causes an interband coupling of the heavy-hole (HH) and light-hole (LH) states but the intraband coupling of these states is zero], but for near resonance with  $E_1$  transitions, the two factors in the denominator of expression (1) resonate at the same time because the intraband coupling does play a role. The observation of  $A_1$ -type phonons in the  $XY$  configuration, when exciting near resonance with

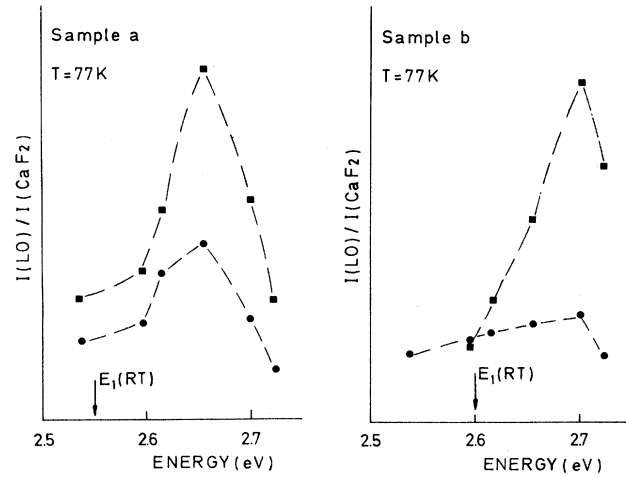


FIG. 5. Scattering intensity of the LO1 and LO2 phonons as a function of the energy of the incident radiation: ●, LO1; ■, LO2. The energy position of the  $E_1$  transition at room temperature is also indicated. The lines are guides to the eye.

the fundamental band-gap transition, has been attributed to band mixing between the LH and HH bands which allows the Fröhlich-interband scattering (impurity induced).<sup>14</sup> Resonating near the fundamental band gap, such a mechanism is observable because the levels are closer in energy, but when resonating in the  $E_1$  region the two valence-band states are distant from each other and, consequently, such a scattering mechanism will not resonate here. It should be pointed out that there are two fourth-order mechanisms able to produce the same selection rules as the Fröhlich interaction, namely the impurity-induced and electric-field-induced mechanisms, and their intensity can be even higher than that induced by Fröhlich interaction.

Summarizing, we have studied the resonance behavior of InAs/AlAs strained-layer superlattices near the  $E_1$  transition. Both types of phonons of InAs ( $A_1$  and  $B_2$ ) resonate in these conditions. This behavior is different from that found when resonating with the fundamental gap  $E_0$ . The different resonance behavior of the two types of phonons with the  $E_1$  and  $E_0$  gaps shows the existence of different electron-phonon interaction mechanisms ruling each resonance.

We thank L. Gonzalez and A. Ruiz for growing the samples.

<sup>1</sup>B. Jusserand, P. Voisin, M. Voos, L. L. Chang, E. E. Méndez, and L. Esaki, Appl. Phys. Lett. **46**, 678 (1985).

<sup>2</sup>F. Cerdeira, A. Pinczuk, J. C. Bean, B. Batlogg, and B. A. Wilson, Appl. Phys. Lett. **45**, 1138 (1989).

<sup>3</sup>G. Armelles, M. Recio, A. Ruiz, and F. Briones, Solid State Commun. **71**, 431 (1989).

<sup>4</sup>J. E. Zucker, A. Pinczuk, D. S. Chemla, A. Gossard, and W. Wiegmann, Phys. Rev. Lett. **51**, 1293 (1983).

<sup>5</sup>A. K. Sood, J. Menéndez, M. Cardona, and K. Ploog, Phys. Rev. Lett. **54**, 2111 (1985).

<sup>6</sup>F. Cerdeira, A. Pinczuk, T. H. Chiu, and W. T. Tsang, Phys. Rev. B **32**, 1390 (1985).

<sup>7</sup>C. Tejedor, J. M. Calleja, F. Meseguer, E. E. Méndez, C. A. Chang, and L. Esaki, Phys. Rev. B **32**, 5303 (1985).

<sup>8</sup>P. V. Santos, A. K. Sood, M. Cardona, K. Ploog, Y. Ohmori, and H. Okamoto, Phys. Rev. B **37**, 6381 (1988).

- <sup>9</sup>F. Briones, L. González, and A. Ruiz, *Appl. Phys. A* (to be published).
- <sup>10</sup>A. K. Sood, J. Menéndez, M. Cardona, and K. Ploog, *Phys. Rev. Lett.* **54**, 2115 (1985).
- <sup>11</sup>E. Richter and D. Strauch, *Solid State Commun.* **64**, 867 (1987).
- <sup>12</sup>Shang-Fen Ren, Hanyou Chu, and Yia-Chung Chang, *Phys. Rev. B* **37**, 8899 (1988).
- <sup>13</sup>W. Hayes and R. Loudon, *Scattering of Light by Crystals* (Wiley, New York, 1978).
- <sup>14</sup>A. Alexandrou, M. Cardona, and K. Ploog, in *Proceedings of the Nineteenth International Conference on the Physics of Semiconductors, Warsaw, Poland*, edited by W. Zawadski (Polish Academy of Sciences, Warsaw, 1988).